Research Article

Academic Platform Journal of Engineering and Smart Systems (APJESS) 11(3), 184-190, 2023
Received: 26-Aug-2023 Accepted: 26-Sep-2023
homepage: https://dergipark.org.tr/tr/pub/apjess
https://doi.org/10.21541/apjess.1350442

Synchronization of Incommensurate Fractional-Order King Cobra Chaotic System

[1]Haris CALGAN, *[2]Abdullah GOKYILDIRIM

[1] Department of Electrical and Electronics Engineering, Balikesir University, Balikesir, Turkey, haris.calgan@balikesir.edu.tr
[2] Department of Electrical and Electronics Engineering, Bandirma Onyedi Eylul University, Balikesir, Turkey, agokyildirim@bandirma.edu.tr

Abstract

In this study, the incommensurate fractional-order King Cobra (IFKC) chaotic system has been investigated. Through bifurcation diagrams and Lyapunov exponent spectra, it has been determined that the IFKC system exhibits rich dynamics. Subsequently, using the Proportional Tilt Integral Derivative (P-TID) control method, synchronization of two IFKC chaotic systems with different initial values has been achieved. Upon examination of the obtained simulation results, it has been demonstrated that the identified IFKC chaotic system and the P-TID controller can be effectively utilized for secure communication.

Keywords: Incommensurate Fractional-Order; Chaos; Synchronization; TID Control

1. INTRODUCTION

The foundations of fractional calculus were laid approximately 300 years ago. Fractional-order analysis offers new perspectives for observing, modeling, and controlling the nature around us [1]. For this reason, many systems in fields such as physics [2], engineering [3], mathematical biology [4], health [5], computer science [6], and more can be described with the help of fractional derivatives.

Chaos theory has been meticulously examined and studied by numerous researchers since Lorenz's work in 1963. Particularly, the study of chaos in fractional dynamic systems in recent years has become an interesting topic. Therefore, fractional-order analyses have been carried out on well-known systems such as Lorenz, Chua, Chen, Rössler, Rucklidge, investigating chaotic behaviors [7-11].

After demonstrating that the dynamic behaviors of chaotic systems can be further diversified through fractional analysis, many researchers have explored the control and synchronization of fractional chaotic systems. The synchronization of chaotic systems forms the basis of chaotic masking, a chaotic-based secure communication method. Therefore, in chaotic masking, which is one of the chaotic-based secure communication methods, synchronization and control play a crucial role. The fundamental aim of synchronization is to ensure that two chaotic systems exhibit the same dynamic behavior after a certain period of time, facilitated by a designed controller. In the literature, various classical methods have been employed for controlling or synchronizing chaotic systems, such as fractional-order PID [12], sliding mode [13], or optimal controllers [14]. Additionally, for the synchronization of chaotic systems, methods like time-delay feedback [15], active [16], passive [17], and adaptive control methods [18], linear quadratic regulator [19] as well as Lyapunov's direct control method [20], have been used.

When examining synchronization studies in the literature, it is observed that many studies involving fractional-order chaotic systems have utilized the commensurate fractional-order method. However, it has been reported that more complex chaotic behaviors can be obtained through incommensurate fractional-order analysis [21]. In this study, an analysis of the previously unexplored incommensurate behavior of the fractional-order King Cobra chaotic system [22] has been conducted. Chaotic behaviors have been identified using bifurcation diagrams and Lyapunov spectra. Moreover, synchronization of two chaotic systems has been achieved using the P-TID controllers, which is not widely employed in the literature for chaos control and synchronization.

The organization of this paper is structured as follows: In Section 2, the dynamic analysis of IFKC chaotic system is conducted using bifurcation diagrams and Lyapunov spectra. In Section 3, two IFKC chaotic systems with different initial conditions are synchronized using the P-TID control method. Finally, conclusions are drawn in Section 4.

2. DYNAMIC ANALYSES OF THE IFKC SYSTEM

Factional derivatives and integrals have gained significance in engineering and mathematics, proving invaluable for scientists and researchers engaged in practical, real-world applications. One widely recognized fractional operator is Caputo's fractional derivative, introduced by Caputo in 1967 and applied in this paper. In the context of both continuous-time and discrete-time systems, the utilization of Caputo's differential operator facilitates the establishment of initial conditions for initial-value problems. The Caputo’s derivative with starting point 0, of order q is defined as below [23]:

$$D^q x = J^{m-q} x^m \tag{1}$$

Here, m represents the integer closest to q, with m>q, and J^a denotes the a^{th} order Riemann-Liouville integral operator, expressed as [24]

$$J^a y = \frac{1}{\Gamma(a)} \int_0^t (t-\tau)^{a-1} y(\tau) d\tau \tag{2}$$

where $\Gamma(.)$ is the Euler’s gamma function. Using the q^{th} order Caputo fractional derivative, the King Cobra system is defined as follows

$$\begin{cases} D^{q_1} x_1(t) = a(y-x) + byz^2 \\ D^{q_2} y_1(t) = cx + dxz^2 \\ D^{q_3} z_1(t) = hz + k|x_1| \end{cases} \tag{3}$$

where parameters a, b, c, d, h, and k are set to 10, 1, 5, -1, -5, and -6. Based on the theorem that defines the requisite condition for the existence of a double-scroll attractor in fractional-order systems [25], the system (3) demonstrates chaotic behavior when the commensurate fractional-order q value exceeds 0.8849 [22]. Hereby, if (3) is considered as commensurate fractional-order while $q_1=q_2=q_3=0.95$, the 2D phase portraits of the system are shown in Figure 1.

As illustrated in Figure 1, the system (3) is verified as a chaotic attractor and y-z phase portrait looks like a face of King Cobra at angry. However, the study in reference [22] has investigated the King Cobra chaotic system only by commensurate fractional-order analysis. In this study, the incommensurate fractional-order analysis is employed to discover a new chaotic response in the King Cobra system which has not been previously studied for this particular system. The effects of the incommensurate orders on the King Cobra chaotic system are investigated. The primary objective is to add dynamic richness to the system by selecting distinct fractional orders for each state equation. Hereby, the system involves more parameters to be adjusted in order to identify a wider range of chaotic behaviors. The bifurcation diagram is evaluated firstly, when ‘a’ is set as bifurcation parameters and incommensurate fractional orders q_1, q_2, q_3 are selected as 0.96, 0.97, 0.98, respectively. The bifurcation diagram of the system (3) is plotted in Figure 2 setting the initial conditions (x_0, y_0, z_0) = (0.1 ,1, 0.1) and change the parameter $a \in [4, 8]$.

It can be seen that when a is between 5.45 and 7.05, the incommensurate fractional-order system is in chaotic state. Setting the system parameter a=7, the initial value $[x_0, y_0, z_0]$=[0.1, 1, 0.1] and q_1=0.96, q_2=0.97, q_3=0.98 the Lyapunov exponent is obtained as drawn in Figure 3. Note that the extended Benettion-Wolf algorithm for incommensurate fractional-order systems is used to determine Lyapunov exponents [26]. As highlighted in Refs. [23] and [26], the result of Lyapunov spectra depends highly on the Gramm-Schmidt coefficient in the algorithm. In this study, the Gramm-Schmidt coefficient is chosen as 0.9 with an integration step of 0.01. The corresponding Lyapunov exponents are obtained as L_1=0.44, L_2=-0.03, L_3=-13.21. The system exhibits chaotic behavior in this case due to the presence of Lyapunov exponents as (+, 0, -) [27].

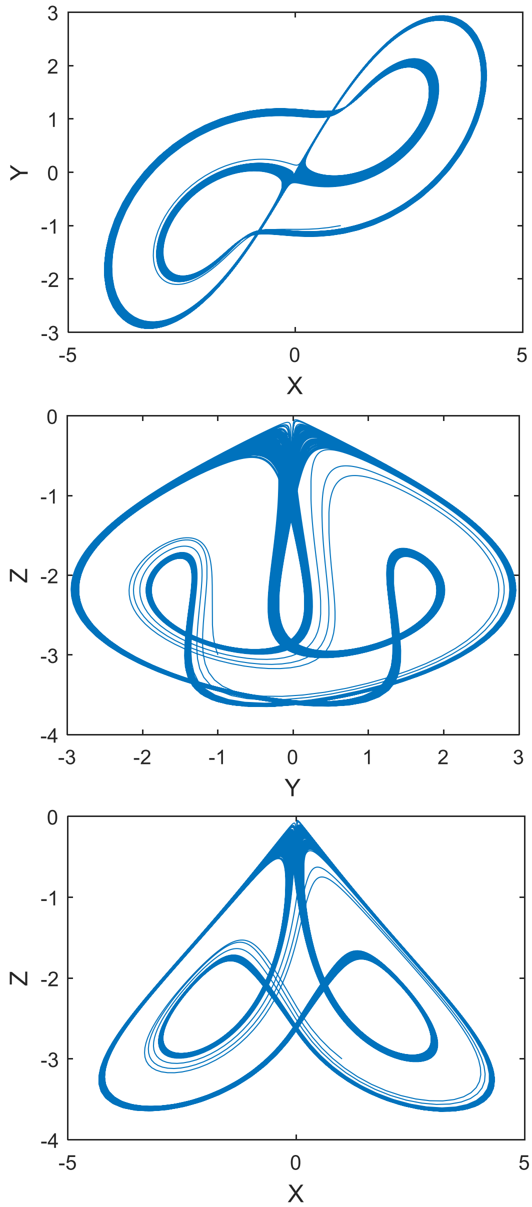

Figure 1. Phase planes of the system (3) when $q_1=q_2=q_3=0.95$, a=6, b=1, c=5, d=-1, h=-5 and k=-6.

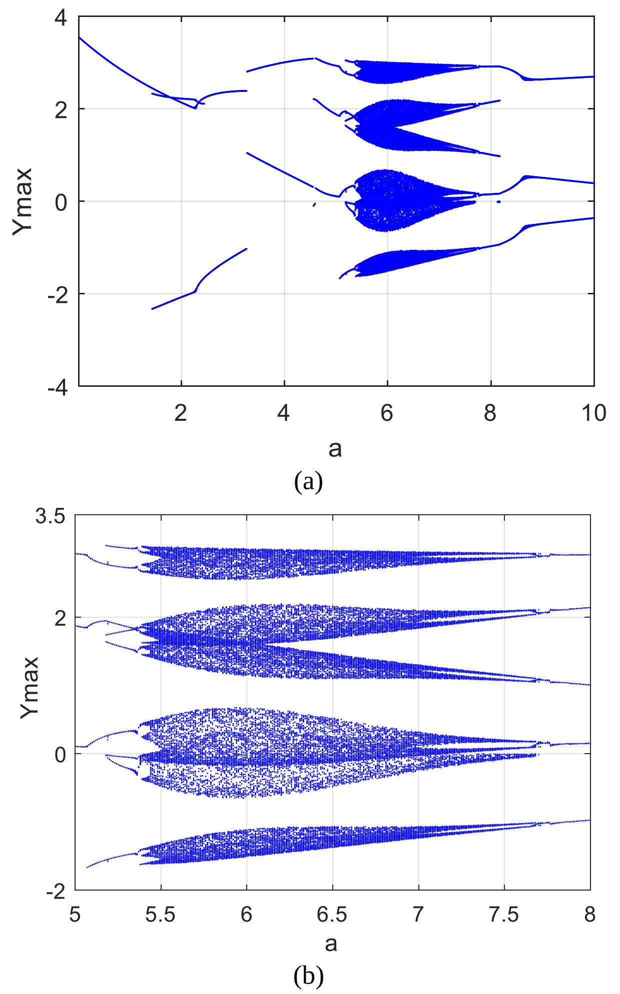

Figure 2. Bifurcation diagram of the system (3) when q_1=0.96, q_2=0.97, q_3=0.98, b=1, c=5, d=-1, h=-5, k=-6 and (a) $a \in [0,10]$, (b) $a \in [5,8]$.

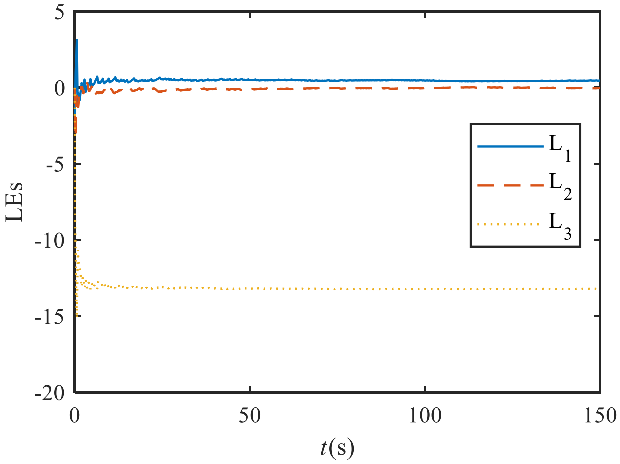

Figure 3. Lyapunov spectra of the system (3) when q_1=0.96, q_2=0.97, q_3=0.98, a=7, b=1, c=5, d=-1, h=-5 and k=-6.

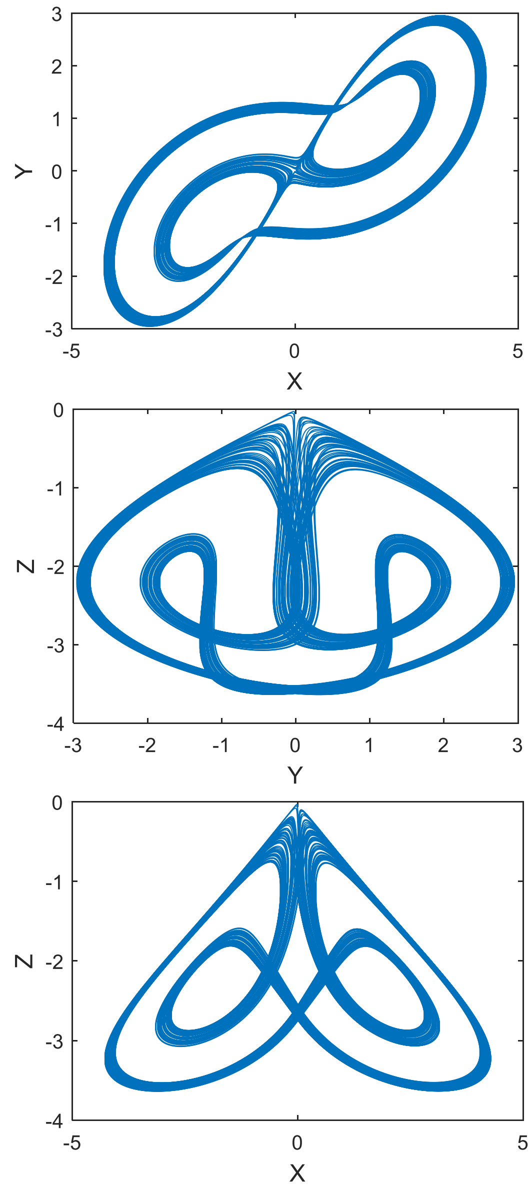

Figure 4. Phase planes of the system (3) when q_1=0.96, q_2=0.97, q_3=0.98, a=7, b=1, c=5, d=-1, h=-5 and k=-6.

Based on the incommensurate fractional-order analysis outcomes derived from bifurcation diagram and Lyapunov spectra, chaotic sequences are obtained by assigning the particular values to the system parameter a=7 and q_1=0.96, q_2=0.97, q_3=0.98. In Figure 4, phase portraits obtained by corresponding bifurcation diagram and Lyapunov spectra is provided. It is demonstrated through phase portraits that the Lyapunov exponent spectra are consistent with bifurcation diagram. The varying incommensurate fractional-order of equations has significant impact on the dynamic characteristics of the system. Consequently, more complex dynamic behaviors become observable when the system orders are incommensurate.

3. SYNCHRONIZATION

In chaos-based secure communication systems, the chaotic masking method is widely employed [20]. In this method, the signal generated by the chaotic system is added to the information signal and transmitted over a certain communication channel. On the receiver side, a second chaotic system is also operated. The signal generated by secondary chaotic system operating on the receiver is subtracted from the incoming information signal to obtain the data. However, if the secondary chaotic system successfully synchronizes with the primary chaotic system, the information signal is obtained correctly. Therefore, chaotic synchronization has attracted the attention of many researchers and plays a crucial role, especially in chaotic masking methods. The purpose of synchronization is to ensure that the two chaotic systems in both the receiver and transmitter exhibit the same dynamic behavior once they are synchronized [28]. In this study, the synchronization of two distinct IFKC systems with different initial conditions has been realized using the P-TID controller.

3.1. P-TID Controller

The TID controller is one of the fractional-order control structures. In this structure, which combines fractional-order control with the classical PID controller, there is a tilted fraction known as the tilted factor. It is known that with the inclusion of the tilt component, the P-TID controller exhibits better tracking dynamics and is more effective against disturbances [29]. Therefore, the P-TID controller has been preferred in this study. The general function of the P-TID controller in the Laplace domain is provided in Eq. (4) [30].

$$G_C = k_p + k_t s^{-1/n} + k_i s^{-1} + k_d s \tag{4}$$

In the given equation, the controller parameters k_p, k_t, k_i, k_d, are respectively the gains of the tilt, integral, and derivative components. In the tilt component given by $s^{-1/n}$, the coefficient n is a real positive number and is usually chosen between 2 and 3.

3.2. Design of error system

After defining the controller, two IFKC systems, each with distinct initial conditions, are established, wherein secondary system requires synchronization with the primary system. The primary and secondary systems are denoted with subscripts 1 and 2, respectively. The primary system is formulated as below:

$$\begin{cases} D^{q_1} x_1(t) = a(y_1 - x_1) + b y_1 z_1^{\,2} \\ D^{q_2} y_1(t) = c x_1 + d x_1 z_1^{\,2} \\ D^{q_3} z_1(t) = h z_1 + k|x_1| \end{cases} \tag{5}$$

Then, the secondary system is specified as follows:

$$\begin{cases} D^{q_1} x_2(t) = a(y_2 - x_2) + b y_2 z_2^{\,2} + u_1 \\ D^{q_2} y_2(t) = c x_2 + d x_2 z_2^{\,2} + u_2 \\ D^{q_3} z_2(t) = h z_2 + k|x_2| + u_3 \end{cases} \tag{6}$$

where u_1, u_2, u_3 are control signals to be designed. Synchronization errors are calculated by subtracting state responses of secondary system from primary system as $e_1=x_1-x_2$, $e_2=y_1-y_2$ and $e_3=z_1-z_2$. Consequently, the error system takes the form as defined below:

$$\begin{cases} D^{q_1} e_1(t) = a(e_2 - e_1) + b(y_1 z_1^{\,2} - y_2 z_2^{\,2}) - u_1 \\ D^{q_2} e_2(t) = c e_1 + d(x_1 z_1^{\,2} - x_2 z_2^{\,2}) - u_2 \\ D^{q_3} e_3(t) = h e_3 + k(|x_1| - |x_2|) - u_3 \end{cases} \tag{7}$$

In this synchronization design, each state is synchronized by distinct P-TID controllers defined by u_1, u_2 and u_3. The aim is to minimize e_1, e_2 and e_3, since the controllers are activated so that both systems given in (5) and (6) are synchronized.

3.3. Numerical Simulations

As detailed in dynamic analysis, incommensurate fractional-orders q_1, q_2, q_3 are selected 0.96, 0.97 and 0.98, respectively. The controller parameters are determined by trial-error method and the best tracking dynamics are observed while k_p, k_t, k_i and k_d parameters are chosen as 1.5, 0. 1, 0.7, 0.5 respectively. The tilted factor n is set to 0.15. Note that, each P-TID controller is equivalent but takes distinct error signals as input and controller parameters are determined by a trial-and-error method.

To demonstrate the synchronization of the system (7), numerical simulations are carried out using the MATLAB program [31]. Note that, despite Caputos’s derivate is employed in dynamical analysis, the synchronization studies use the memory principle of Grünwald-Letnikow fractional-order solver definition code provided in [32] with a fixed step size t_{step}=5e-3. Prior to synchronization, the initial conditions for the primary and secondary systems are set as $x_1(0)=0.1$, $y_1(0)=1$, $z_1(0)=0.1$ and $x_2(0)=0$, $y_2(0)=-0.5$, $z_2(0)=0$, respectively. During the numerical simulations, the P-TID controllers are activated at t(s)=20, initiating the synchronization process. The synchronization error functions $e_x(t)$, $e_y(t)$ and $e_z(t)$ are depicted in Figure 5.

As anticipated, the corresponding Figure 5 shows the successful control achieved by the designed P-TID controller over the synchronization of IFKC chaotic system. After the controllers are activated at t(s)=20, all of the error functions go to zero which yields effective synchronization as illustrated in Figure 6.

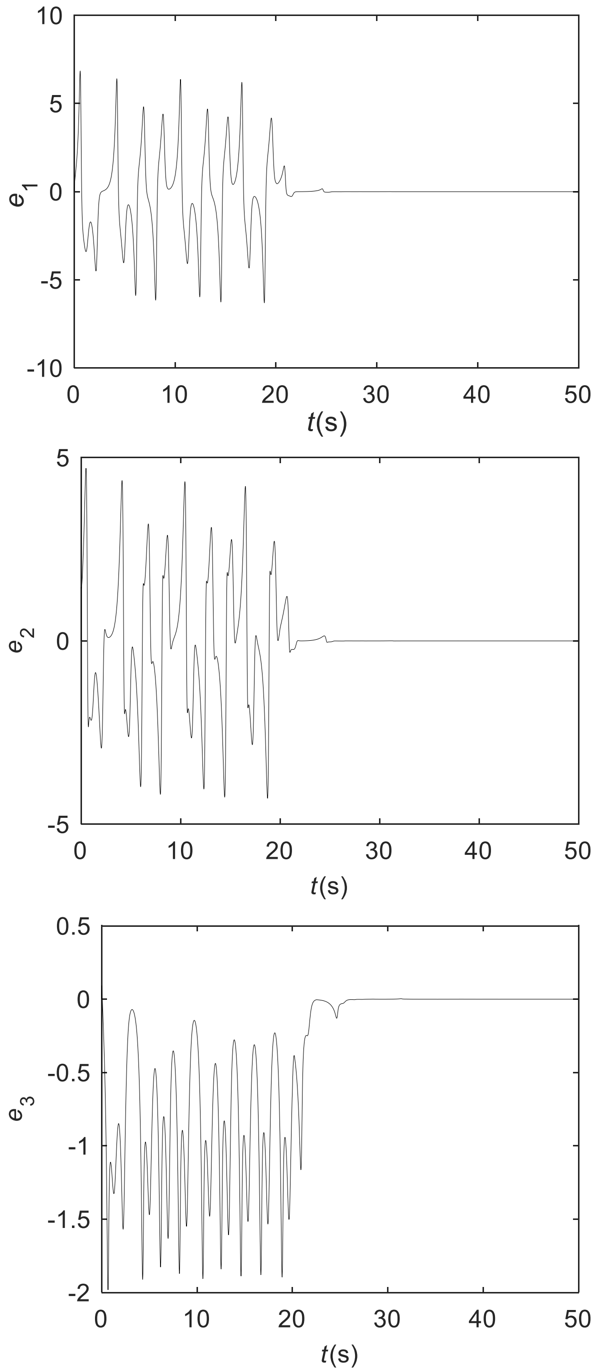

Figure 5. Error functions e_x (t), e_y (t) and e_z (t) of P-TID based synchronization.

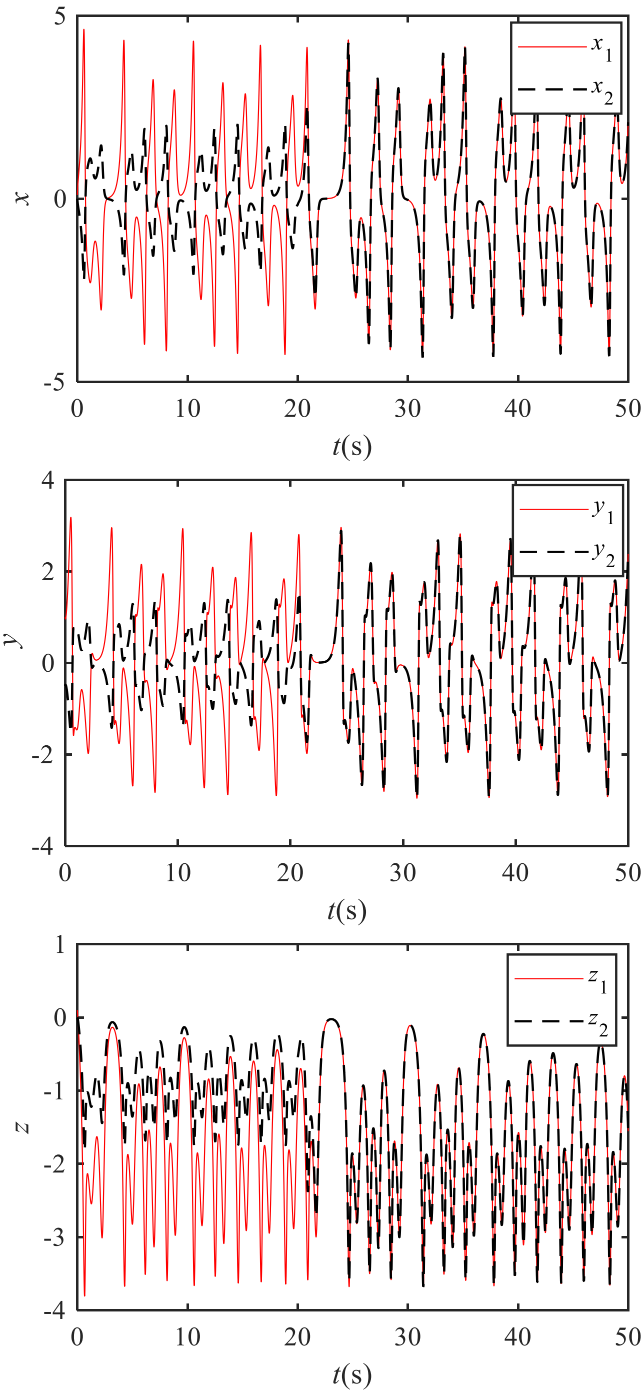

Figure 6. Time series of P-TID-based synchronization.

4. CONCLUSION

In this study, incommensurate fractional-order analysis of King Cobra system is realized. The increased dynamic diversity is contributed by the varying fractional-order values of the presented system. Points of chaos in the system due to parameter changes are identified through bifurcation diagram analyses and Lyapunov spectra. Due to these analyses, more complex chaotic behavior is observed when fractional-orders are chosen as q_1=0.96, q_2=0.97 and q_3=0.98. Later, two IFKC chaotic systems, each initialized with distinct initial conditions, are synchronized. In this context, the secondary system achieves synchronization with the primary system through the utilization of a P-TID controller. The obtained time series of P-TID-based synchronization demonstrate that the established system can be employed for further secure communication studies. However, controller performance may be improved through future research using optimization methods.

Author contributions: Concept – H.C., A.G.; Data Collection & Processing – H.C., A.G.; Literature Search – H.C., A.G.; Writing – H.C., A.G.
Conflict of Interest: No conflict of interest was declared by the authors.
Financial Disclosure: The authors declared that this study has received no financial support.

REFERENCES

[1] M. Demirtas, E. Ilten, and H. Calgan, "Pareto-based multi-objective optimization for fractional order PI^{λ} speed control of induction motor by using Elman Neural Network," Arab. J. Sci. Eng., vol. 44, no. 3, pp. 2165–2175, 2019.

[2] Z. Wei, A. Akgul, U. E. Kocamaz, I. Moroz, and W. Zhang, "Control, electronic circuit application and fractional-order analysis of hidden chaotic attractors in the self-exciting homopolar disc dynamo," Chaos, Solitons & Fractals, vol. 111, pp. 157–168, 2018.

[3] E. Ilten and M. Demirtas, "Fractional order super-twisting sliding mode observer for sensorless control of induction motor," COMPEL - Int. J. Comput. Math. Electr. Electron. Eng., vol. 38, no. 2, pp. 878–892, Mar. 2019.

[4] M. Odabaşı, "Exact analytical solutions of the fractional biological population model, fractional EW and modified EW equations," An Int. J. Optim. Control Theor. Appl., vol. 11, no. 1, pp. 52–58, 2021.

[5] A. A. Hamou, R. R. Q. Rasul, Z. Hammouch, and N. Özdemir, "Analysis and dynamics of a mathematical model to predict unreported cases of COVID-19 epidemic in Morocco," Comput. Appl. Math., vol. 41, no. 6, p. 289, 2022.

[6] D. Avcı and F. Soytürk, "Optimal control strategies for a computer network under virus threat," J. Comput. Appl. Math., vol. 419, p. 114740, 2023.

[7] I. Grigorenko and E. Grigorenko, "Chaotic dynamics of the fractional Lorenz system," Phys. Rev. Lett., vol. 91, no. 3, p. 34101, 2003.

[8] T. T. Hartley, C. F. Lorenzo, and H. K. Qammer, "Chaos in a fractional order Chua's system," IEEE Trans. Circuits Syst. I Fundam. Theory Appl., vol. 42, no. 8, pp. 485–490, 1995.

[9] A. Gokyildirim, H. Calgan, and M. Demirtas, "Fractional-Order sliding mode control of a 4D memristive chaotic system," J. Vib. Control, p. 10775463231166188, 2023.

[10] A. Akgul, C. Arslan, and B. Arıcıoglu, "Design of an interface for random number generators based on integer and fractional order chaotic systems," Chaos Theory Appl., vol. 1, no. 1, pp. 1–18, 2019.

[11] A. Akgul, Y. Adiyaman, A. Gokyildirim, B. Aricioglu, M. A. Pala, and M. E. Cimen, "Electronic circuit implementations of a fractional-order chaotic system and observing the escape from chaos," J. Circuits, Syst. Comput., vol. 32, no. 05, p. 2350085, Mar. 2023.

[12] O. Atan, M. Turk, and R. Tuntas, "Fractional order controller design for fractional order chaotic synchronization.," Int. J. Nat. Eng. Sci., vol. 7, no. 3, 2013.

[13] G. Xu, S. Zhao, and Y. Cheng, "Chaotic synchronization based on improved global nonlinear integral sliding mode control☆," Comput. Electr. Eng., vol. 96, p. 107497, 2021.

[14] F. Motallebzadeh, M. R. J. Motlagh, and Z. R. Cherati, "Synchronization of different-order chaotic systems: Adaptive active vs. optimal control," Commun. Nonlinear Sci. Numer. Simul., vol. 17, no. 9, pp. 3643–3657, 2012.

[15] C. Ge, C. Hua, and X. Guan, "Master-slave synchronization criteria of Lur'e systems with time-delay feedback control," Appl. Math. Comput., vol. 244, pp. 895–902, 2014.

[16] S. Çiçek, A. Ferikoglu, and I. Pehlivan, "A new 3D chaotic system: Dynamical analysis, electronic circuit design, active control synchronization and chaotic masking communication application," Optik (Stuttg)., vol. 127, no. 8, pp. 4024–4030, 2016.

[17] S. Keyong, B. Ruixuan, G. Wang, W. Qiutong, and Z. Yi, "Passive synchronization control for integer-order chaotic systems and fractional-order chaotic systems," in 2019 Chinese Control Conference (CCC), 2019, pp. 1115–1119.

[18] Z.-A. S. A. Rahman, H. A. A. Al-Kashoash, S. M. Ramadhan, and Y. I. A. Al-Yasir, "Adaptive control synchronization of a novel memristive chaotic system for secure communication applications," Inventions, vol. 4, no. 2, p. 30, 2019.

[19] P. Alexander, S. Emiroğlu, S. Kanagaraj, A. Akgul, and K. Rajagopal, "Infinite coexisting attractors in an autonomous hyperchaotic megastable oscillator and linear quadratic regulator-based control and synchronization," Eur. Phys. J. B, vol. 96, no. 1, p. 12, 2023.

[20] A. Gokyildirim, U. E. Kocamaz, Y. Uyaroglu, and H. Calgan, "A novel five-term 3D chaotic system with cubic nonlinearity and its microcontroller-based secure communication implementation," AEU - Int. J. Electron. Commun., vol. 160, p. 154497, Feb. 2023.

[21] C. Ma, J. Mou, J. Liu, F. Yang, H. Yan, and X. Zhao, "Coexistence of multiple attractors for an incommensurate fractional-order chaotic system," Eur. Phys. J. Plus, vol. 135, pp. 1–21, 2020.

[22] P. Muthukumar, P. Balasubramaniam, and K. Ratnavelu, "Synchronization and an application of a novel fractional order King Cobra chaotic system," Chaos An Interdiscip. J. Nonlinear Sci., vol. 24, no. 3, 2014.

[23] A. Gokyildirim, “Circuit realization of the fractional-order Sprott K chaotic system with standard components,” Fractal Fract., vol. 7, no. 6, p. 470, 2023.

[24] K. Rajagopal et al., “Multistability and coexisting attractors in a new circulant chaotic system,” Int. J. Bifurc. Chaos, vol. 29, no. 13, p. 1950174, 2019.

[25] M. S. Tavazoei and M. Haeri, “A necessary condition for double scroll attractor existence in fractional-order systems,” Phys. Lett. A, vol. 367, no. 1–2, pp. 102–113, 2007.

[26] M.-F. Danca, “Matlab code for Lyapunov exponents of fractional-order systems, part ii: The noncommensurate case,” Int. J. Bifurc. Chaos, vol. 31, no. 12, p. 2150187, 2021.

[27] A. Wolf, J. B. Swift, H. L. Swinney, and J. A. Vastano, “Determining Lyapunov exponents from a time series,” Phys. D Nonlinear Phenom., vol. 16, no. 3, pp. 285–317, Jul. 1985.

[28] S. Emiroglu, A. Akgül, Y. Adıyaman, T. E. Gümüş, Y. Uyaroglu, and M. A. Yalçın, “A new hyperchaotic system from T chaotic system: dynamical analysis, circuit implementation, control and synchronization,” Circuit World, vol. 48, no. 2, pp. 265–277, 2022.

[29] H. Calgan and M. Demirtas, “Design and implementation of fault tolerant fractional order controllers for the output power of self-excited induction generator,” Electr. Eng., vol. 103, no. 5, pp. 2373–2389, 2021.

[30] T. Amieur, M. Bechouat, M. Sedraoui, S. Kahla, and H. Guessoum, “A new robust tilt-PID controller based upon an automatic selection of adjustable fractional weights for permanent magnet synchronous motor drive control,” Electr. Eng., pp. 1–18, 2021.

[31] S. Matlab, “Matlab,” MathWorks, Natick, MA, 2012.

[32] H. Li, Y. Shen, Y. Han, J. Dong, and J. Li, “Determining Lyapunov exponents of fractional-order systems: A general method based on memory principle,” Chaos, Solitons & Fractals, vol. 168, p. 113167, 2023.